Mononuclear and Mixed-Valence Trinuclear Manganese Complexes Containing Tripodal Tetradentate Ligands. Phenolato, Carboxylato, and Alkoxo Bridges

Masakazu Hirotsu,* Masaaki Kojima, and Yuzo Yoshikawa

Department of Chemistry, Faculty of Science, Okayama University, Tsushima, Okayama 700

(Received October 21, 1996)

Manganese complexes containing tripodal tetradentate ligands with an N_2O_2 donor set (H_2L^1: *N*,*N*-bis(2-hydroxybenzyl)-*N*′,*N*′-dimethylethylenediamine, H_2L^2: *N*-(3,5-di-*t*-butyl-2-hydroxybenzyl)-*N*-(2-hydroxybenzyl)-*N*′,*N*′-dimethylethylenediamine, H_2L^3: *N*,*N*-bis(3,5-di-*t*-butyl-2-hydroxybenzyl)-*N*′,*N*′-dimethylethylenediamine) have been prepared. The mononuclear and trinuclear complexes with the additional carboxylate ligand were isolated. The steric effect of the 3-positioned *t*-butyl groups on the aromatic rings of the tripodal ligand controls the type of the complex structure. The L^3 ligand gave a mononuclear complex, [Mn(L^3)(mcba)(CH_3OH)], where mcba is a *m*-chlorobenzoate anion; the structure has been determined by X-ray analysis. The trinuclear complexes are formulated as [$Mn_3(L^n)_2$(carboxylato)$_2(OCH_3)_2$] (n = 1, 2). For the L^4 and L^5 ligands (H_2L^4: *N*,*N*-bis(5-methoxy-2-hydroxybenzyl)-*N*′,*N*′-dimethylethylenediamine, H_2L^5: *N*,*N*-bis(5-chloro-2-hydroxybenzyl)-*N*′,*N*′-dimethylethylenediamine), trinuclear complexes were also obtained. Three trinuclear complexes were also structurally characterized by X-ray analysis. The three manganese cores are arranged linearly, and the structural parameters indicate that the oxidation states are Mn^{III}–Mn^{II}–Mn^{III}. The Mn^{III} and Mn^{II} cores are bridged by phenolate, carboxylate, and alkoxide groups, and the manganese cores are separated in the range of 3.14 and 3.17 Å. The variable-temperature magnetic susceptibility measurements of the mixed-valence trinuclear complexes revealed that the spin exchange coupling constants (J) between Mn^{III} and Mn^{II} ions range from −0.25 to 1.9 cm^{-1}. The exchange interactions are weak, and both antiferromagnetic and ferromagnetic interactions were observed.

A polynuclear manganese complex is found to be involved in redox active enzymes.[1] It is thought that the active center for water oxidation in photosystem II consists of an oxo bridged polynuclear manganese complex.[2—8] Manganese complexes bridged by oxo ligands have been synthesized for various polydentate ligands. In particular, the manganese Schiff base complexes with an N_2O_2 donor set have been extensively studied.[9—16] The manganese complexes containing the *N*,*N*′-propane-1,3-bis(salicylideneaminate) derivatives are the most well-studied ones. The Mn^{IV}–Mn^{IV} di-μ-oxo dinuclear complexes have been obtained by oxygenation reactions of either manganese(II) Schiff base complexes with dioxygen[12—14] or manganese(III) Schiff base complexes with hydrogen peroxide or *t*-butyl peroxide.[9] In each case, the reaction mechanism was proposed. In order to verify the mechanism of those reactions, a complex with a tripodal tetradentate ligand is suitable because the ligand requires a rigid geometry and the remaining two cis positions can be used for the formation of the di-μ-oxo bridges. However, the manganese complex containing the tripodal ligand with an N_2O_2 donor set has never been established. Thus we initiated the study of the manganese complex with an N_2O_2 tripodal ligand.

In this report, we describe the preparation of mononuclear and trinuclear manganese complexes containing tripodal tetradentate ligands with an N_2O_2 donor set. In order to control the steric and electronic effect of the coordination environment, several kinds of functional groups were introduced to the aromatic rings of the ligand. The structures of a mononuclear and three trinuclear complexes were determined by X-ray analysis. The trinuclear complexes consist of the central Mn^{II} core and the flanking Mn^{III} cores, and the three manganese cores are arranged linearly. The Mn^{III} and Mn^{II} cores are bridged by phenolate, carboxylate, and alkoxide groups. For the mixed-valence trinuclear complexes, the temperature-dependent magnetic behavior was examined.

Experimental

The following abbreviations are used for carboxylic acids: Hba = benzoic acid; Hmcba = *m*-chlorobenzoic acid; Hpmba = *p*-methoxybenzoic acid; Hbf = benzoylformic acid.

Ligands. Abbreviations of the tripodal tetradentate ligands are represented in Chart 1. All ligands were prepared by a modification of the method reported by Hinshaw et al.[17] A representative procedure is given for *N*-(3,5-di-*t*-butyl-2-hydroxybenzyl)-*N*-(2-hydroxybenzyl)-*N*′,*N*′-dimethylethylenediamine (H_2L^2).

3,5-Di-*t*-butylsalicylaldehyde (2.34 g, 10 mmol) was dissolved in warm methanol (10 cm^3). A methanol solution (10 cm^3) of *N*,*N*-dimethylethylenediamine (0.88 g, 10 mmol) was added to the solution with stirring. The resulting yellow solution was refluxed for 2 h. After cooling the solution, $NaBH_4$ (1.13 g, 30 mmol) was slowly added with stirring. The solution was stirred at room temperature for an additional 5 h to give a colorless solution. The solvent was removed, and the residue was taken up in a 0.1 M (1 M = 1 mol dm^{-3}) NaOH aqueous solution (100 cm^3). The solution

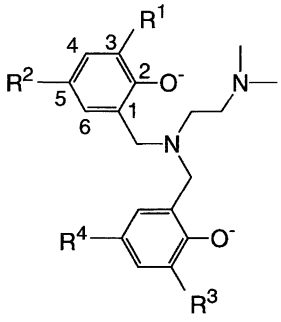

	R^1	R^2	R^3	R^4
L^1	H	H	H	H
L^2	*t*-Bu	*t*-Bu	H	H
L^3	*t*-Bu	*t*-Bu	*t*-Bu	*t*-Bu
L^4	H	OCH_3	H	OCH_3
L^5	H	Cl	H	Cl

Chart 1.

was extracted with CH_2Cl_2 (60 cm^3, 2×70 cm^3), and the extracts were washed with water (2×100 cm^3) and dried over Na_2SO_4. The solvent was removed to give a colorless oil. This product was *N*-(3,5-di-*t*-butyl-2-hydroxybenzyl)-*N'*,*N'*-dimethylethylenediamine (a quantitative yield). The oil was dissolved in methanol (100 cm^3), and a methanol solution (20 cm^3) of salicylaldehyde (1.22 g, 10 mmol) was added. The resulting light yellow solution was neutralized with a methanolic HCl solution. $NaBH_3CN$ (1.26 g, 20 mmol) was slowly added to the solution with stirring. The solution was stirred for 22 h at room temperature. The solvent was removed, and the light yellow residue was taken up in a 0.1 M NaOH aqueous solution (100 cm^3). The solution was extracted with CH_2Cl_2 (60 cm^3, 2×70 cm^3), and the extracts were washed with water (2×100 cm^3) and dried over Na_2SO_4. After filtration, methanol (50 cm^3) was added to the extracts. The solution was concentrated by rotary evaporation and allowed to stand. After 2 d, a crystalline product was deposited, collected by filtration, and washed with methanol. Recrystallization was carried out from dichloromethane–methanol to give colorless needles. The yield was 1.56 g (38%). ^{1}H NMR ($CDCl_3$) δ = 1.26 (s, 9H), 1.36 (s, 9H), 2.32 (s, 6H), 2.59 (s, 4H), 3.59 (s, 2H), 3.66 (s, 2H), 6.72—7.21 (m, 6H).

[Mn(L^3)(mcba)(CH_3OH)] (1). To a solution of $MnCl_2 \cdot 4H_2O$ (0.059 g, 0.3 mmol) in methanol (10 cm^3) was added H_2L^3 (0.157 g, 0.3 mmol) to give a light purple suspension. A 0.1 M solution (6 cm^3, 0.6 mmol) of NaOH in methanol was added dropwise with stirring, and the suspension was stirred for 1 h. To the resulting deep purple solution was added *m*-chlorobenzoic acid (0.047 g, 0.3 mmol), and the solution was stirred. A purple microcrystalline solid was deposited. After stirring for an additional 1 h, the precipitate was collected by filtration and washed with methanol. The crude product was recrystallized from dichloromethane-methanol to yield 0.155 g (68%) of **1**. IR (KBr pellet) ν_{as} (COO) 1604, ν_s (COO) 1367 cm^{-1}. μ_{eff} (298 K) 4.79 μ_B. Found: C, 65.69; H, 8.01; N, 3.64%. Calcd for $C_{42}H_{62}ClMnN_2O_5$: C, 65.91; H, 8.17; N, 3.66%. A piece of the crystal was used for the X-ray crystal structure determination.

[$Mn_3(L^1)_2$(mcba)$_2$(OCH_3)$_2$]·2CH_2Cl_2 (2). The H_2L^1 ligand (0.210 g, 0.7 mmol) was added to a solution of $Mn(ClO_4)_2 \cdot 6H_2O$ (0.507 g, 1.4 mmol) in methanol (15 cm^3). To this solution was added *m*-chlorobenzoic acid (0.219 g, 1.4 mmol), and the reaction mixture was stirred. A 0.5 M solution (5.6 cm^3, 2.8 mmol) of NaOH in methanol was added dropwise with stirring, and the solution turned dark green. After stirring for 5 h, a dark green solid was precipitated, collected by filtration, and washed with methanol. The crude product was recrystallized from dichloromethane–methanol to yield 0.181 g (40%) of **2**. IR (KBr pellet) ν_{as}(COO) 1594, ν_s(COO) 1388 cm^{-1}. μ_{eff} (298 K, per Mn_3 molecule) 9.12 μ_B. Found: C, 49.89; H, 4.71; N, 4.34%. Calcd for $C_{54}H_{62}Cl_6Mn_3N_4O_{10}$: C, 49.71; H, 4.79; N, 4.29%. A piece of the crystal was used for the X-ray crystal structure determination.

[$Mn_3(L^1)_2$(ba)$_2$(OCH_3)$_2$] (3). This complex was prepared by the same method as that for [$Mn_3(L^1)_2$(mcba)$_2$(OCH_3)$_2$] except that benzoic acid was used instead of *m*-chlorobenzoic acid. Yield: 49%. IR (KBr pellet) ν_{as}(COO) 1596, ν_s(COO) 1394 cm^{-1}. μ_{eff} (298 K, per Mn_3 molecule) 9.01 μ_B. Found: C, 57.95; H, 5.53; N, 5.27%. Calcd for $C_{52}H_{60}Mn_3N_4O_{10}$: C, 58.60; H, 5.67; N, 5.26%.

[$Mn_3(L^1)_2$(bf)$_2$(OCH_3)$_2$] (4). The H_2L^1 ligand (0.150 g, 0.5 mmol) was added to a solution of $MnCl_2 \cdot 6H_2O$ (0.099 g, 0.5 mmol) in methanol (10 cm^3). A methanol solution (5 cm^3) of *N*,*N*-diisopropylethylamine (0.194 g, 1.5 mmol) was added dropwise with stirring. The resulting dark brown solution was stirred for 1 h. To this solution was added benzoylformic acid (0.075 g, 0.5 mmol), and the reaction mixture was stirred for 3 h. The resulting brown precipitate was collected by filtration and washed with methanol. Recrystallization was carried out from dichloromethane–methanol. The yield was 0.087 g (47%). μ_{eff} (298 K, per Mn_3 molecule) 8.92 μ_B. Found: C, 57.47; H, 5.75; N, 5.47%. Calcd for $C_{54}H_{60}Mn_3N_4O_{12}$: C, 57.81; H, 5.39; N, 4.99%. A piece of the crystal was used for the X-ray crystal structure determination.

[$Mn_3(L^2)_2$(mcba)$_2$(OCH_3)$_2$] (5). This complex was prepared by the same method as that for [$Mn_3(L^1)_2$(mcba)$_2$(OCH_3)$_2$] except that H_2L^2 was used instead of H_2L^1. Yield: 60%. IR (KBr pellet) ν_{as}(COO) 1598, ν_s(COO) 1386 cm^{-1}. μ_{eff} (298 K, per Mn_3 molecule) 9.24 μ_B. Found: C, 59.70; H, 6.59; N, 4.08%. Calcd for $C_{68}H_{90}Cl_2Mn_3N_4O_{10}$: C, 60.09; H, 6.67; N, 4.12%.

[$Mn_3(L^2)_2$(ba)$_2$(OCH_3)$_2$]·CH_2Cl_2 (6). This complex was prepared by the same method as that for [$Mn_3(L^2)_2$(mcba)$_2$(OCH_3)$_2$] except that benzoic acid was used instead of *m*-chlorobenzoic acid. Yield: 67%. IR (KBr pellet) ν_{as}(COO) 1599, ν_s(COO) 1394 cm^{-1}. μ_{eff} (298 K, per Mn_3 molecule) 9.21 μ_B. Found: C, 60.59; H, 6.76; N, 4.16%. Calcd for $C_{69}H_{94}Cl_2Mn_3N_4O_{10}$: C, 60.26; H, 6.89; N, 4.07%.

[$Mn_3(L^4)_2$(pmba)$_2$(OCH_3)$_2$] (7). This complex was prepared by the same method as that for [$Mn_3(L^1)_2$(mcba)$_2$(OCH_3)$_2$] except that H_2L^4 and *p*-methoxybenzoic acid were used instead of H_2L^1 and *m*-chlorobenzoic acid. Yield: 40%. IR (KBr pellet) 1606, 1598, ν_s(COO) 1390 cm^{-1}. μ_{eff} (298 K, per Mn_3 molecule) 8.94 μ_B. Found: C, 55.18; H, 5.76; N, 4.44%. Calcd for $C_{58}H_{72}Mn_3N_4O_{16}$: C, 55.91; H, 5.82; N, 4.50%.

[$Mn_3(L^5)_2$(mcba)$_2$(OCH_3)$_2$]·2CH_3OH (8). This complex was prepared by the same method as that for [$Mn_3(L^1)_2$(mcba)$_2$(OCH_3)$_2$] except that H_2L^5 was used instead of H_2L^1. Yield: 65%. IR (KBr pellet) ν_{as}(COO) 1592, ν_s(COO) 1387 cm^{-1}. μ_{eff} (298 K, per Mn_3 molecule) 8.97 μ_B. Found: C, 48.31; H, 5.14; N, 4.57%. Calcd for $C_{54}H_{62}Cl_6Mn_3N_4O_{12}$: C, 48.52; H, 4.68; N, 4.19%.

[Mn(L^3)(acac)] (9). To a solution of $MnCl_2 \cdot 4H_2O$ (0.099 g, 0.5 mmol) in methanol (15 cm^3) was added H_2L^3 (0.262 g, 0.5

mmol) to give a light purple suspension. A 0.5 M solution (2 cm^3, 1.0 mmol) of NaOH in methanol was added dropwise with stirring, and the suspension was stirred for 1 h. To the resulting deep purple solution was added a methanol solution (10 cm^3) of acetylacetone (0.100 g, 1 mmol), and the solution was stirred for an additional 1 h. The volume of the purple solution was reduced by rotary evaporation and allowed to stand. A purple crystalline product was deposited, collected by filtration, and washed with cold methanol. The crude product was recrystallized from dichloromethane–methanol to yield 0.209 g (62%) of **9**. μ_{eff} (298 K) 4.78 μ_B. Found: C, 69.12; H, 9.05; H, 4.18%. Calcd for $C_{39}H_{61}MnN_2O_4$: C, 69.21; H, 9.08; N, 4.14%.

[Mn(L^5)(acac)] (10). The H_2L^5 ligand (0.185 g, 0.5 mmol) was added to a solution of $Mn(ClO_4)_2 \cdot 6H_2O$ (0.181 g, 0.5 mmol) in ethanol (10 cm^3). To the resulting deep brown solution was added an ethanol solution (5 cm^3) of acetylacetone (0.100 g, 1 mmol) and *N,N*-diisopropylethylamine (0.129 g, 1.5 mmol), and the solution was stirred for 1 h. The resulting dark brown solution was allowed to stand. Dark brown needles were deposited, collected by filtration, and washed with ethanol. Recrystallization was carried out from dichloromethane–ethanol. The yield was 0.178 g (68%) of **10**. μ_{eff} (298 K) 4.80 μ_B. Found: C, 52.69; H, 5.04; N, 5.59%. Calcd for $C_{23}H_{27}Cl_2MnN_2O_4$: C, 52.99; H, 5.22; N, 5.37%.

Physical Measurements. Visible-UV absorption spectra were recorded with a JASCO Ubest-550 spectrophotometer. Infrared spectra were recorded with a JASCO IR-810 and an ATI Mattson Galaxy FTIR 3000 spectrophotometer. Magnetic susceptibility data in the 2—270 K temperature range were collected using a high-sensitivity Faraday balance with a superconducting magnet (Oxford Instruments, Inc.). The values of the applied magnetic field strength were as follows: 0.15 T (the temperature range: 2—20 K), 1.08 T (20—269 K) for **3**; 0.15 T (2—20 K), 0.86 T (20—253 K) for **5**; 0.21 T (2—20 K), 1.08 T (20—256 K) for **6**; 1.08 T (2—260 K) for **7**. Room-temperature magnetic susceptibilities were measured with a Sherwood Scientific LTD Model MK1 magnetic susceptibility balance. The susceptibilities were corrected for diamagnetism estimated from Pascal's constants. ^{1}H NMR spectra were measured at 270 MHz on a JEOL EX-270 spectrometer.

Collection and Reduction of X-Ray Data. Crystallographic data are given in Table 1. All calculations were carried out using the TEXSAN[18] crystallographic software package on a Silicon Graphics IRIS Indigo workstation. For the following complexes, the structures were solved by direct methods (SHELXS 86)[19] and expanded using Fourier techniques. The non-hydrogen atoms were refined anisotropically by a full-matrix least-squares procedure.

[Mn(L^3)(mcba)(CH_3OH)] (1). A purple prismatic crystal (0.50×0.25×0.50 mm) was mounted on a Rigaku AFC-5S diffractometer. The cell parameters were obtained by a least-squares refinement of the angular settings of 25 reflections in the range of $21° < 2\theta < 23°$. Data collections were carried out using graphite-monochromated Mo $K\alpha$ radiation to a maximum 2θ value of 52.1°. The intensities of three standard reflections were measured after every 97 reflections and showed no significant reduction during the data collection. An empirical absorption correction based on ψ scans of three reflections was applied. In the structure refinement, hydrogen atoms were included except for that bonded to the oxygen of the coordinated methanol molecule, but not refined, and were placed at fixed distances of 0.95 Å from bonded carbon atoms. The maximum and minimum peaks on the final difference Fourier map corresponded to 0.63 and −0.52 e $Å^{-3}$, respectively.

[$Mn_3(L^1)_2$(mcba)$_2$(OCH_3)$_2$]·2CH_2Cl_2 (2). A brown prismatic crystal (0.25×0.17×0.30 mm) was mounted on an Enraf–Nonius CAD-4 diffractometer. The cell parameters were obtained by a least-squares refinement of the angular settings of 25 reflections in the range of $20° < 2\theta < 42°$. Intensity data were collected using graphite-monochromated Mo $K\alpha$ radiation to a maximum

Table 1. Crystallographic Data for [Mn(L^3)(mcba)(CH_3OH)] (**1**), [$Mn_3(L^1)_2$(mcba)$_2$(OCH_3)$_2$]·2CH_2Cl_2(**2**), [$Mn_3(L^2)_2$(mcba)$_2$-(OCH_3)$_2$] (**5**), and [$Mn_3(L^1)_2$(bf)$_2$(OCH_3)$_2$] (**4**)

	1	2	5	4
Formula	$C_{42}H_{62}ClMnN_2O_5$	$C_{54}H_{62}Cl_6Mn_3N_4O_{10}$	$C_{68}H_{90}Cl_2Mn_3N_4O_{10}$	$C_{54}H_{60}Mn_3N_4O_{12}$
Fw	765.35	1304.64	1359.20	1121.90
Crystal system	Triclinic	Triclinic	Monoclinic	Orthorhombic
Space group	$P\bar{1}$ (No. 2)	$P\bar{1}$ (No. 2)	$P2_1/c$ (No. 14)	$P2_12_12_1$ (No. 19)
a/Å	13.782(3)	11.771(2)	13.412(2)	20.156(3)
b/Å	16.590(4)	12.236(3)	14.192(1)	21.039(5)
c/Å	9.589(1)	12.486(2)	19.151(4)	12.700(5)
α/deg	102.80(2)	64.27(2)		
β/deg	99.07(1)	64.88(1)	106.52(1)	
γ/deg	95.39(2)	84.31(2)		
V/$Å^3$	2092.3(8)	1458.8(6)	3494.8(8)	5385(2)
Z	2	1	2	4
D_{calcd}/g cm^{-3}	1.215	1.485	1.292	1.384
λ/Å	0.7107 (Mo $K\alpha$)	0.7107 (Mo $K\alpha$)	0.7107 (Mo $K\alpha$)	0.7107 (Mo $K\alpha$)
μ/cm^{-1}	4.22	9.72	6.67	7.56
T/°C	25	25	25	25
No. of total data collected	8748	6608	8095	5868
No. of unique data	8230	6314	7872	
No. of observations	4543 ($I > 3\sigma(I)$)	3812 ($I > 3\sigma(I)$)	4003 ($I > 3\sigma(I)$)	2730 ($I > 2.7\sigma(I)$)
No. of variables	460	474	394	658
R[a]	0.056	0.042	0.047	0.047
R_w[b]	0.036	0.041	0.046	0.027

a) $R = \sum||F_o| - |F_c||/\sum|F_o|$. b) $R_w = [\sum w(|F_o| - |F_c|)^2/\sum wF_o^2]^{1/2}$, $w = 1/\sigma^2(F_o)$.

2θ value of 53.9°. The intensities of three standard reflections were monitored after every two hours; a 3.04% decay was observed during the data collection. The data were scaled to correct for this effect. An empirical absorption correction based on ψ scans of three reflections was applied. In the structure refinement, hydrogen atoms were refined isotropically except for those of the dichloromethane molecule. The maximum and minimum peaks on the final difference Fourier map corresponded to 0.52 and −0.51 e Å^{-3}, respectively.

$[Mn_3(L^2)_2(mcba)_2(OCH_3)_2]$ (5). A brown prismatic crystal (0.40×0.18×0.40 mm) was mounted on an Enraf–Nonius CAD-4 diffractometer. The cell parameters were obtained by a least-squares refinement of the angular settings of 21 reflections in the range of $20° < 2\theta < 42°$. Intensity data were collected using graphite-monochromated Mo $K\alpha$ radiation to a maximum 2θ value of 53.9°. The intensities of three standard reflections were measured after every two hours and showed no significant reduction during the data collection. An empirical absorption correction based on ψ scans of three reflections was applied. In the structure refinement, hydrogen atoms were included, but not refined, and were placed at fixed distances of 0.95 Å from bonded carbon atoms. The maximum and minimum peaks on the final difference Fourier map corresponded to 0.73 and −0.45 eÅ^{-3}, respectively.

$[Mn_3(L^1)_2(bf)_2(OCH_3)_2]$ (4). A brown plate (0.22×0.05×0.43 mm) was mounted on a Rigaku AFC-5R diffractometer. The cell parameters were obtained by a least-squares refinement of the angular settings of 25 reflections in the range of $19° < 2\theta < 23°$. Data collections were carried out using graphite-monochromated Mo $K\alpha$ radiation to a maximum 2θ value of 52.0°. The intensities of three standard reflections were measured after every 97 reflections and showed no significant reduction during the data collection. An empirical absorption correction based on ψ scans of three reflections was applied. In the structure refinement, hydrogen atoms were included, but not refined, and were placed at fixed distances of 0.95 Å from bonded carbon atoms. The maximum and minimum peaks on the final difference Fourier map corresponded to 0.41 and −0.38 eÅ^{-3}, respectively.

For the above four complexes, full crystallographic data, experimental details, atomic coordinates and equivalent isotropic temperature factors for all atoms, anisotropic temperature factors for non-hydrogen atoms, complete bond distances and angles, tables of observed and calculated structure factors, and fully labeled ORTEP diagrams are deposited as Document No. 70009 at the Office of the Editor of Bull. Chem. Soc. Jpn.

Results and Discussion

Mononuclear Manganese Complex with a Carboxylate Ligand. The L^3 ligand has four *t*-butyl groups on the aromatic rings. The *t*-butyl groups exert an electron-donating effect on the phenolate oxygen donor atom and a large steric effect. In particular, the 3-positioned *t*-butyl groups prevent the formation of a polynuclear complex. Clearly the L^3 ligand is the bulkiest among the five tripodal ligands studied here. A carboxylate ligand is useful for the study of the polynuclear complex because of the variety of the coordination modes. A manganese(II) ion coordinated by the tripodal ligand is oxidized to manganese(III) species in air. Introduction of a carboxylate group to the manganese cation containing the L^3 ligand gave only the mononuclear complex, $[Mn(L^3)(mcba)(CH_3OH)]$ (**1**). The effective magnetic moment of this complex is 4.79 μ_B. This value is in agreement with the spin-only value (4.90 μ_B) for a high-spin manganese(III) ion.

Figure 1 shows a perspective view of the structure of $[Mn(L^3)(mcba)(CH_3OH)]$ (**1**). The selected bond distances and angles are given in Table 2. The *m*-chlorobenzoate ligand acts as a monodentate ligand. The manganese(III) center is in a distorted octahedral environment. Two phenolate oxygen donors and the tertiary amine nitrogen of the tripodal ligand and a carboxylate oxygen donor of *m*-chlorobenzoate form an equatorial plane. The terminal nitrogen occupies an axial position, and the remaining axial site is occupied by a methanol molecule. The equatorial Mn–N bond distance of 2.098(3) Å is comparable to those reported for other manganese(III) complexes containing equatorial Mn^{III}–N(amine) bonds.[20] The two Mn–O(phenolato) distances of 1.865(3) and 1.896(3) Å are located within the range of those for manganese(III) complexes reported. The Mn–O(carboxylato) bond of 1.999(3) Å is slightly longer than those of the equatorial Mn^{III}–O bonds of μ-acetato bridges reported for

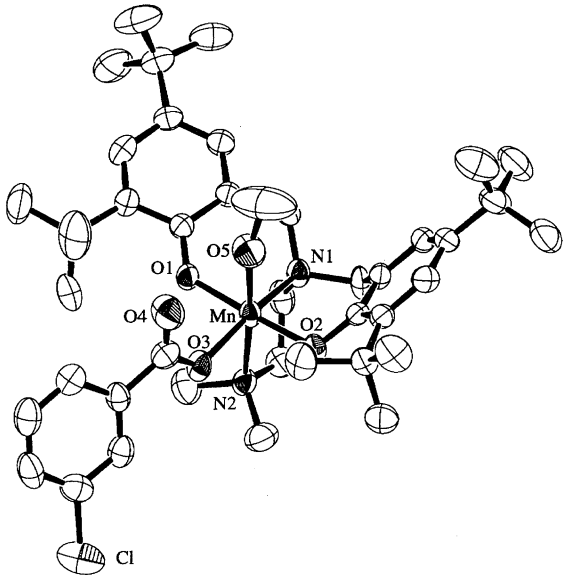

Fig. 1. ORTEP diagram of $[Mn(L^3)(mcba)(CH_3OH)]$ (**1**).

Table 2. Selected Bond Distances (Å) and Angles (deg) for $[Mn(L^3)(mcba)(CH_3OH)]$ (**1**)

Mn–O(1)	1.865(3)	Mn–O(2)	1.896(3)
Mn–O(3)	1.999(3)	Mn–O(5)	2.268(3)
Mn–N(1)	2.098(3)	Mn–N(2)	2.355(4)
O(5)···O(4)	2.597(5)		
O(1)–Mn–O(2)	177.2(1)	O(1)–Mn–O(3)	89.8(1)
O(1)–Mn–O(5)	87.1(1)	O(1)–Mn–N(1)	87.7(1)
O(1)–Mn–N(2)	91.1(1)	O(2)–Mn–O(3)	92.4(1)
O(2)–Mn–O(5)	91.1(1)	O(2)–Mn–N(1)	90.6(1)
O(2)–Mn–N(2)	90.9(1)	O(3)–Mn–O(5)	91.4(1)
O(3)–Mn–N(1)	165.0(1)	O(3)–Mn–N(2)	84.2(1)
O(5)–Mn–N(1)	103.2(1)	O(5)–Mn–N(2)	175.2(1)
N(1)–Mn–N(2)	81.1(1)		

manganese polynuclear complexes.[21—23] The axial bond distances of 2.268(3) Å for Mn–O5 and 2.355(4) Å for Mn–N2 are larger than those in the equatorial plane. This is consistent with a Jahn–Teller distortion of this high-spin d^4 compound. The distance between the uncoordinated carboxylate oxygen (O4) and the oxygen (O5) of the coordinated methanol molecule is 2.597(5) Å. This short distance indicates that a hydrogen bond exists between O4 and the hydrogen bound to O5.

Trinuclear Complexes with Carboxylate Bridges. The phenolate oxygen donors of the tripodal ligands, L^1, L^2, L^4, and L^5, can act as bridging sites to give polynuclear complexes. For these ligands, trinuclear manganese complexes with carboxylate bridges were isolated. Generally, the trinuclear complexes were prepared by the reaction of $Mn(ClO_4)_2 \cdot 6H_2O$ (2 equiv) with a tripodal ligand (1 equiv), carboxylic acid (2 equiv), and NaOH or *N,N*-diisopropylethylamine (4 equiv) in methanol. However, the reaction of 1 equiv of $Mn(ClO_4)_2 \cdot 6H_2O$ for the tripodal ligand gave the same product. On the other hand, for the L^3 ligand, no trinuclear complex was obtained under similar conditions.

The structure of $[Mn_3(L^1)_2(mcba)_2(OCH_3)_2]$ (**2**) is shown in Fig. 2. The selected bond distances and angles are given in Table 3. The central metal (Mn2) is located on a crystallographic inversion center. The two flanking metals (Mn1 and Mn1*) are coordinated by the L^1 ligands. These cores in different environments are bridged by phenolate, carboxylate, and alkoxide groups. Thus, the central manganese is coordinated octahedrally by six oxygen donors. The Mn2–O distances are 2.246(2) for Mn2–O2(phenolato), 2.177(2) for Mn2–O4(carboxylato), and 2.180(2) Å for Mn2–O5(alkoxo). These values are typical for those between a manganese(II) ion and the oxygen donors. On the other hand, the lengths of the coordination bonds of two terminal cores with the tripodal ligands are similar to those of the mononuclear manganese(III) complex, $[Mn(L^3)(mcba)(CH_3OH)]$. However, the Mn1–O2(bridged phenolato) bond distance of 1.947(2) Å is slightly larger than the Mn1–O1(non-bridged phenolato) distance (1.872(2) Å) and the distances of Mn–O(phenolato) for $[Mn(L^3)(mcba)(CH_3OH)]$ (**1**). The axial bond distances, Mn–O3 (2.198(2) Å) and Mn–N2 (2.390(3) Å), are clearly longer than those in the equatorial plane as observed in mononuclear manganese(III) complexes. On the basis of the above observations, the oxidation state of the central core (Mn2) is assigned to Mn^{II}, and those of the flanking cores are assigned to Mn^{III}. These assignments are supported by analysis of the variable-temperature magnetic susceptibility (vide infra).

Table 3. Selected Bond Distances (Å) and Angles (deg) for $[Mn_3(L^1)_2(mcba)_2(OCH_3)_2] \cdot 2CH_2Cl_2$ (**2**)

Mn(1)–O(1)	1.872(2)	Mn(1)–O(2)	1.947(2)
Mn(1)–O(3)	2.198(2)	Mn(1)–O(5)	1.900(2)
Mn(1)–N(1)	2.110(3)	Mn(1)–N(2)	2.390(3)
Mn(2)–O(2)	2.246(2)	Mn(2)–O(4)	2.177(2)
Mn(2)–O(5)	2.180(2)	Mn(1)···Mn(2)	3.1720(7)
O(1)–Mn(1)–O(2)	175.4(1)	O(1)–Mn(1)–O(3)	92.2(1)
O(1)–Mn(1)–O(5)	92.7(1)	O(1)–Mn(1)–N(1)	92.0(1)
O(1)–Mn(1)–N(2)	90.5(1)	O(2)–Mn(1)–O(3)	87.9(1)
O(2)–Mn(1)–O(5)	82.7(1)	O(2)–Mn(1)–N(1)	92.6(1)
O(2)–Mn(1)–N(2)	90.3(1)	O(3)–Mn(1)–O(5)	95.7(1)
O(3)–Mn(1)–N(1)	87.3(1)	O(3)–Mn(1)–N(2)	167.3(1)
O(5)–Mn(1)–N(1)	174.3(1)	O(5)–Mn(1)–N(2)	96.5(1)
N(1)–Mn(1)–N(2)	80.2(1)	O(2)–Mn(2)–N(4)	88.87(9)
O(2)–Mn(2)–O(5)	70.07(8)	O(4)–Mn(2)–O(5)	89.05(9)
Mn(1)–O(2)–Mn(2)	98.04(9)	Mn(1)–O(5)–Mn(2)	101.8(1)

Figure 3 shows the structure of $[Mn_3(L^2)_2(mcba)_2(OCH_3)_2]$ (**5**). The selected bond distances and angles are given in Table 4. This structure is very similar to that of $[Mn_3(L^1)_2(mcba)_2(OCH_3)_2]$ (**2**). Therefore, $[Mn_3(L^2)_2(mcba)_2(OCH_3)_2]$ (**5**) is also assigned to a mixed-valence trinuclear complex with the Mn^{III}–Mn^{II}–Mn^{III} arrangement. The oxygen donor of the phenolate group with *t*-butyl groups cannot bridge because of the steric hindrance.

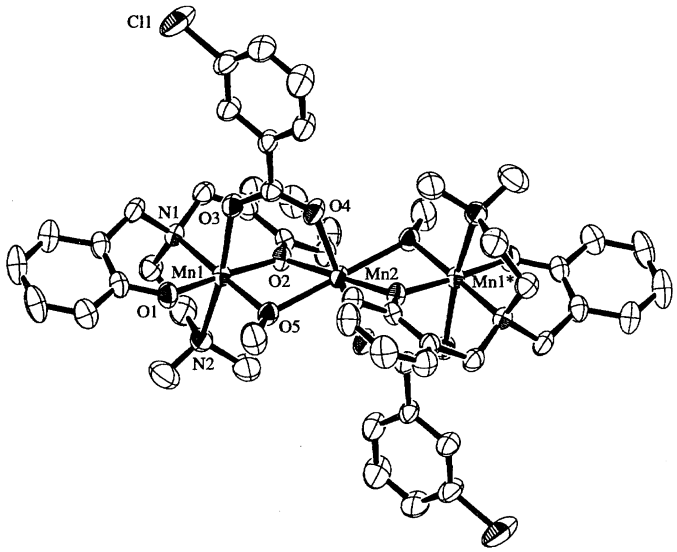

Fig. 2. ORTEP diagram of $[Mn_3(L^1)_2(mcba)_2(OCH_3)_2]$ (**2**).

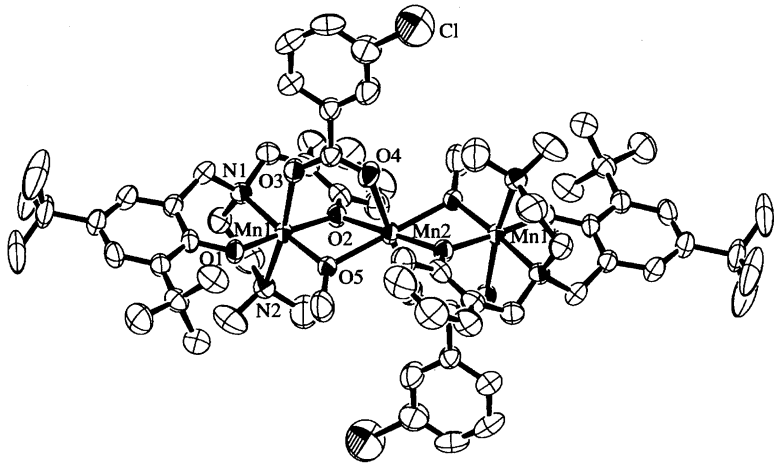

Fig. 3. ORTEP diagram of $[Mn_3(L^2)_2(mcba)_2(OCH_3)_2]$ (**5**).

Table 4. Selected Bond Distances (Å) and Angles (deg) for $[Mn_3(L^2)_2(mcba)_2(OCH_3)_2]$ (**5**)

Mn(1)–O(1)	1.872(3)	Mn(1)–O(2)	1.941(3)
Mn(1)–O(3)	2.219(3)	Mn(1)–O(5)	1.897(3)
Mn(1)–N(1)	2.116(3)	Mn(1)–N(2)	2.428(4)
Mn(2)–O(2)	2.218(3)	Mn(2)–O(4)	2.172(3)
Mn(2)–O(5)	2.156(3)	Mn(1)···Mn(2)	3.1728(6)
O(1)–Mn(1)–O(2)	175.7(1)	O(1)–Mn(1)–O(3)	92.1(1)
O(1)–Mn(1)–O(5)	94.2(1)	O(1)–Mn(1)–N(1)	92.9(1)
O(1)–Mn(1)–N(2)	92.1(1)	O(2)–Mn(1)–O(3)	88.1(1)
O(2)–Mn(1)–O(5)	81.5(1)	O(2)–Mn(1)–N(1)	91.4(1)
O(2)–Mn(1)–N(2)	88.8(1)	O(3)–Mn(1)–O(5)	94.1(1)
O(3)–Mn(1)–N(1)	87.3(1)	O(3)–Mn(1)–N(2)	165.9(1)
O(5)–Mn(1)–N(1)	172.7(1)	O(5)–Mn(1)–N(2)	99.0(1)
N(1)–Mn(1)–N(2)	79.1(1)	O(2)–Mn(2)–O(4)	87.2(1)
O(2)–Mn(2)–O(5)	69.9(1)	O(4)–Mn(2)–O(5)	89.7(1)
Mn(1)–O(2)–Mn(2)	99.2(1)	Mn(1)–O(5)–Mn(2)	102.9(1)

However, little steric effect was observed in this structure.

We examined the reaction with a variety of carboxylic acid derivatives. However, for the tripodal ligands, L^1, L^2, L^4, and L^5, we could not obtain a mononuclear complex with a monodentate carboxylate ligand, such as $[Mn(L^3)(mcba)(CH_3OH)]$ (**1**). The structure of $[Mn_3(L^1)_2(bf)_2(OCH_3)_2]$ (**4**) is shown in Fig. 4. The selected bond distances and angles are given in Table 5. This crystal structure has no crystallographic inversion center, and the Mn^{III}–Mn^{II}–Mn^{III} angle is 175.4(1)°. However, the central Mn^{II} ion (Mn3) is almost the inversion center of the $[Mn_3(L^1)_2(bf)_2(OCH_3)_2]$ molecule. Other structural parameters are similar to the above trinuclear complexes.

All the trinuclear complexes studied here have three bridging ligands: phenolate, carboxylate, and alkoxide groups. For the above three complexes, the average Mn^{III}–O(phenolato)–Mn^{II} angle is 98.9°, and the average Mn^{III}–O(alkoxo)–Mn^{II} angle is 102.4°. These values are smaller than

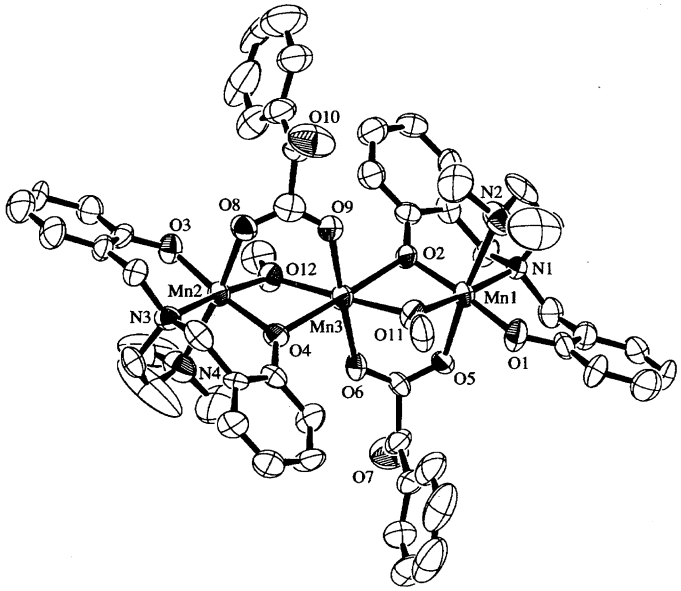

Fig. 4. ORTEP diagram of $[Mn_3(L^1)_2(bf)_2(OCH_3)_2]$ (**4**).

Table 5. Selected Bond Distances (Å) and Angles (deg) for $[Mn_3(L^1)_2(bf)_2(OCH_3)_2]$ (**4**)

Mn(1)–O(1)	1.871(7)	Mn(1)–O(2)	1.926(7)
Mn(1)–O(5)	2.255(7)	Mn(1)–O(11)	1.887(7)
Mn(1)–N(1)	2.090(9)	Mn(1)–N(2)	2.39(1)
Mn(2)–O(3)	1.845(7)	Mn(2)–O(4)	1.928(7)
Mn(2)–O(8)	2.244(8)	Mn(2)–O(12)	1.912(7)
Mn(2)–N(3)	2.080(9)	Mn(2)–N(4)	2.39(1)
Mn(3)–O(2)	2.191(7)	Mn(3)–O(4)	2.205(7)
Mn(3)–O(6)	2.182(8)	Mn(3)–O(9)	2.200(9)
Mn(3)–O(11)	2.136(8)	Mn(3)–O(12)	2.130(8)
Mn(1)···Mn(3)	3.137(3)	Mn(2)···Mn(3)	3.154(3)
Mn(1)···Mn(2)	6.287(2)		
O(1)–Mn(1)–O(2)	174.4(3)	O(1)–Mn(1)–O(5)	89.5(3)
O(1)–Mn(1)–O(11)	92.1(3)	O(1)–Mn(1)–N(1)	92.3(3)
O(1)–Mn(1)–N(2)	89.9(4)	O(2)–Mn(1)–O(5)	88.3(3)
O(2)–Mn(1)–O(11)	82.8(3)	O(2)–Mn(1)–N(1)	92.9(3)
O(2)–Mn(1)–N(2)	93.1(4)	O(5)–Mn(1)–O(11)	91.0(3)
O(5)–Mn(1)–N(1)	89.2(3)	O(5)–Mn(1)–N(2)	170.3(3)
O(11)–Mn(1)–N(1)	175.6(3)	O(11)–Mn(1)–N(2)	98.7(4)
N(1)–Mn(1)–N(2)	81.1(4)	O(3)–Mn(2)–N(4)	173.0(3)
O(3)–Mn(2)–O(8)	87.6(3)	O(3)–Mn(2)–O(12)	92.0(3)
O(3)–Mn(2)–N(3)	93.4(3)	O(3)–Mn(2)–N(4)	91.2(4)
O(4)–Mn(2)–O(8)	89.2(3)	O(4)–Mn(2)–O(12)	81.9(3)
O(4)–Mn(2)–N(3)	92.8(3)	O(4)–Mn(2)–N(4)	93.1(4)
O(8)–Mn(2)–O(12)	93.2(3)	O(8)–Mn(2)–N(3)	88.4(3)
O(8)–Mn(2)–N(4)	169.3(4)	O(12)–Mn(2)–N(3)	174.4(3)
O(12)–Mn(2)–N(4)	97.5(4)	N(3)–Mn(2)–N(4)	81.0(4)
O(2)–Mn(3)–O(4)	177.8(3)	O(2)–Mn(3)–O(6)	89.6(3)
O(2)–Mn(3)–O(9)	90.0(3)	O(2)–Mn(3)–O(11)	71.3(3)
O(2)–Mn(3)–O(12)	108.7(3)	O(4)–Mn(3)–O(6)	92.6(3)
O(4)–Mn(3)–O(9)	87.8(3)	O(4)–Mn(3)–O(11)	109.0(3)
O(4)–Mn(3)–O(12)	70.9(3)	O(6)–Mn(3)–O(9)	177.5(3)
O(6)–Mn(3)–O(11)	87.1(3)	O(6)–Mn(3)–O(12)	95.2(3)
O(9)–Mn(3)–O(11)	90.5(3)	O(9)–Mn(3)–O(12)	87.3(3)
O(11)–Mn(3)–O(12)	177.7(4)	Mn(1)···Mn(3)···Mn(2)	176.30(9)
Mn(1)–O(2)–Mn(3)	99.1(3)	Mn(2)–O(4)–Mn(3)	99.2(3)
Mn(1)–O(11)–Mn(3)	102.3(3)	Mn(2)–O(12)–Mn(3)	102.4(3)

the tetrahedral angle. However, the sum of the bond angles around the bridged oxygen donors is about 360° in both cases, except that the value around the alkoxo oxygen of $[Mn_3(L^1)_2(mcba)_2(OCH_3)_2]$ (**2**) is 352°. The distances between the Mn^{III} and Mn^{II} cores are similar, and the average manganese separation of the three trinuclear complexes is 3.16 Å. In the case of the trinuclear mixed-valence manganese complexes bridged by four carboxylate and two alkoxide groups, the manganese separations are in the range 3.41—3.52 Å and the Mn^{III}–O(alkoxo)–Mn^{II} angle is ca. 120°.[21—23] That is, the manganese separation is mainly dependent on the types of the bridging ligands, and the angle around the alkoxo bridge changes flexibly.

Electronic Spectra of Mononuclear and Trinuclear Complexes. The electronic spectra of the mononuclear and the trinuclear complexes with carboxylate ligands are illustrated in Fig. 5. The mononuclear complex, $[Mn(L^3)(mcba)(CH_3OH)]$ (**1**), shows an absorption band at 19.8×10^3 cm^{-1} ($\varepsilon = 2780$ M^{-1} cm^{-1}). The band is assigned to an LMCT transition from a pπ orbital on the phenolate oxygen to the manganese(III) dπ^* orbitals, as reported for other manganese(III) complexes.[20] The band with the higher intensity at 27.6×10^3 cm^{-1} ($\varepsilon = 4200$ M^{-1} cm^{-1}) is also assigned to another LMCT band. The two similar LMCT bands are observed in $[Mn(L^3)(acac)]$ (**9**), the maxima of the bands being 20.6×10^3 cm^{-1} ($\varepsilon = 2350$ M^{-1} cm^{-1}) and 27.1×10^3 cm^{-1} ($\varepsilon = 4430$ M^{-1} cm^{-1}). On the other hand, $[Mn(L^5)(acac)]$ (**10**) exhibits the former band at 21.5×10^3 cm^{-1} ($\varepsilon = 1600$ M^{-1} cm^{-1}), and the higher energy transition is observed as a shoulder. This shift to higher energy on substitution with an electron-withdrawing group supports the assignment to the phenolate-to-manganese(III) charge transfer transition. In the mixed-valence trinuclear complexes, $[Mn_3(L^1)_2(mcba)_2(OCH_3)_2]$ (**2**), $[Mn_3(L^2)_2(mcba)_2(OCH_3)_2]$ (**5**), $[Mn_3(L^4)_2(pmba)_2(OCH_3)_2]$ (**7**), and $[Mn_3(L^5)_2(mcba)_2(OCH_3)_2]$ (**8**), the LMCT band at ca. 20×10^3 cm^{-1} is absent. Instead, a new band is observed at 22.6—22.8×10^3 cm^{-1}. This band is insensitive to the substitutions of the functional groups on the aromatic ring of the tripodal ligands.

Magnetic Behavior of Trinuclear Complexes. Temperature-dependent molar susceptibility measurements of pow-

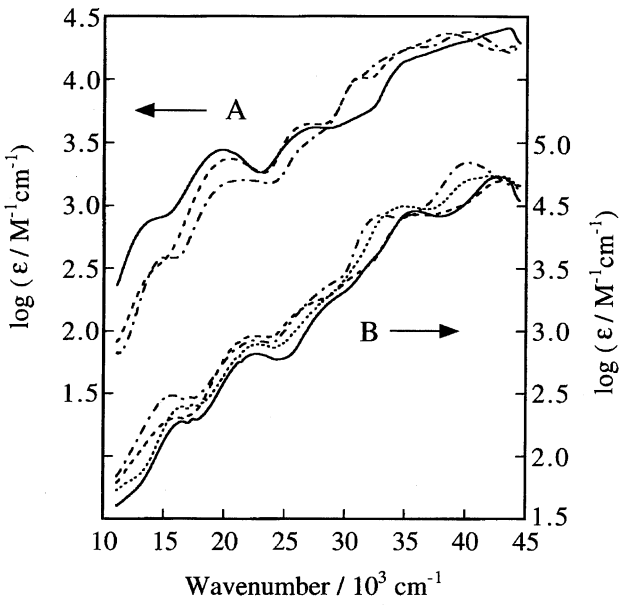

Fig. 5. Electronic spectra of mononuclear (A) and trinuclear (B) complexes in dichloromethane; A: $[Mn(L^3)(mcba)(CH_3OH)]$ (**1**) (—), $[Mn(L^3)(acac)]$ (**9**) (- - -), and $[Mn(L^5)(acac)]$ (**10**) (–·–); B: $[Mn_3(L^1)_2(mcba)_2(OCH_3)_2]$ (**2**) (—), $[Mn_3(L^2)_2(mcba)_2(OCH_3)_2]$ (**5**) (- - -), $[Mn_3(L^4)_2(pmba)_2(OCH_3)_2]$ (**7**) (–·–), and $[Mn_3(L^5)_2(mcba)_2(OCH_3)_2]$ (**8**) (····).

dered samples of trinuclear complexes, $[Mn_3(L^1)_2(ba)_2(OCH_3)_2]$ (**3**), $[Mn_3(L^2)_2(mcba)_2(OCH_3)_2]$ (**5**), $[Mn_3(L^2)_2(ba)_2(OCH_3)_2]$ (**6**), and $[Mn_3(L^4)_2(pmba)_2(OCH_3)_2]$ (**7**), were carried out in the temperature range 2—270 K (Figs. 6 and 7). In $[Mn_3(L^4)_2(pmba)_2(OCH_3)_2]$ (**7**), the effective magnetic moment decreases from 8.97 μ_B at 260 K to 5.73 μ_B at 2.2 K. This indicates an antiferromagnetic coupling

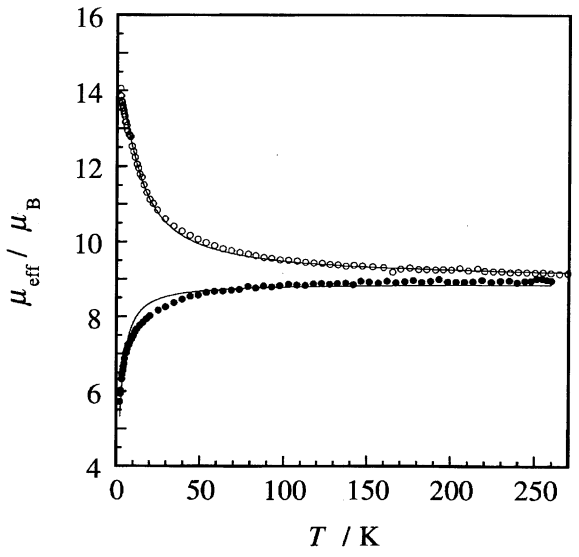

Fig. 6. Temperature dependence of the magnetic moments per molecule of $[Mn_3(L^1)_2(ba)_2(OCH_3)_2]$ (**3**) (○) and $[Mn_3(L^4)_2(pmba)_2(OCH_3)_2]$ (**7**) (●). Solid lines represent the least-squares fits.

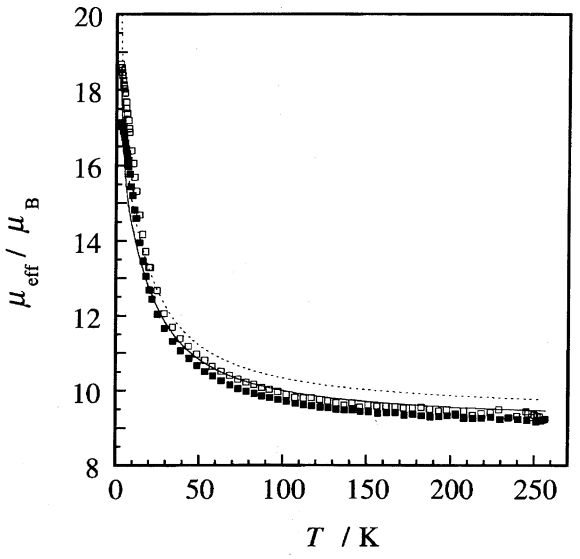

Fig. 7. Temperature dependence of the magnetic moments per molecule of $[Mn_3(L^2)_2(mcba)_2(OCH_3)_2]$ (**5**) (□) and $[Mn_3(L^2)_2(ba)_2(OCH_3)_2]$ (**6**) (■). Dashed and solid lines represent the least-squares fits for **5** and **6**, respectively.

between the electronic spins of two Mn^{III} and one Mn^{II} ions. On the other hand, the effective magnetic moment of $[Mn_3(L^1)_2(ba)_2(OCH_3)_2]$ (**3**) increases from 9.17 μ_B at 269 K to 14.07 μ_B at 2.0 K. This is characteristic of a ferromagnetic spin exchange coupling.

The magnetic data were analyzed using the isotropic spin exchange coupling model. The spin Hamiltonian in linear trinuclear complexes is expressed as

$$H = -2(J_{12}S_1 \cdot S_2 + J_{23}S_2 \cdot S_3 + J_{31}S_3 \cdot S_1),$$

where $S_1=5/2$ and $S_2=S_3=2$ for the S_2–S_1–S_3 arrangement. In the case of the trinuclear complexes studied here, it is assumed that the terminal manganese(III) ions are equivalent. Therefore, the spin exchange coupling constant for the Mn^{III}–Mn^{II} interactions is expressed as $J=J_{12}=J_{31}$. The interaction between the terminal manganese(III) ions is expected to be negligible ($J_{23}=0$). A theoretical expression for the molar magnetic susceptibility is derived using the Kambe vector-coupling method[24] and the Van Vleck equation. The expression has been described in a literature.[25] The curve fittings were employed for two parameters of J and g (the average g value). The minimized function was $\Sigma[(\mu_{eff})_{exptl}-(\mu_{eff})_{calcd}]^2$. The best fits were obtained with $J=-0.25$ cm^{-1} and $g=1.95$ for $[Mn_3(L^4)_2(pmba)_2(OCH_3)_2]$ (**7**); $J=1.05$ cm^{-1} and $g=1.98$ for $[Mn_3(L^1)_2(ba)_2(OCH_3)_2]$ (**3**).

$[Mn_3(L^2)_2(mcba)_2(OCH_3)_2]$ (**5**) and $[Mn_3(L^2)_2(ba)_2(OCH_3)_2]$ (**6**) exhibit the ferromagnetic spin exchange interactions. The effective magnetic moments of these complexes increase from 9.30 μ_B at 253 K to 18.69 μ_B at 2.7 K for $[Mn_3(L^2)_2(mcba)_2(OCH_3)_2]$ (**5**) and from 9.24 μ_B at 256 K to 17.05 μ_B at 2.8 K for $[Mn_3(L^2)_2(ba)_2(OCH_3)_2]$ (**6**). If two $S=2$ ions and one $S=5/2$ ion are completely coupled by intramolecular ferromagnetic interaction, the complex be-

haves as an $S=13/2$ system. In this case, the maximum μ_{eff} should be 13.96 μ_B with $g=2.0$ on the basis of a spin-only equation. Therefore, the larger μ_{eff} values below 15 K suggest that an intermolecular interaction exists. This effect was modeled by introduction of the parameter θ (replacing T in the theoretical expression to $T-\theta$). The best fitting parameters were $J=1.9$ cm^{-1}, $g=2.06$, and $\theta=1.4$ K for $[Mn_3(L^2)_2(mcba)_2(OCH_3)_2]$ (**5**); $J=1.9$ cm^{-1}, $g=2.00$, and $\theta=1.2$ K for $[Mn_3(L^2)_2(ba)_2(OCH_3)_2]$ (**6**).

The formation of similar mixed-valence trinuclear manganese complexes is found for the tridentate Schiff base ligand with an NO_2 donor set.[21—23] In those cases, the Mn^{III} and Mn^{II} are bridged by two carboxylate and one alkoxide groups. The spin exchange coupling constants reported for the trinuclear complexes with the Mn^{III}–Mn^{II}–Mn^{III} arrangement are in the range of -7.1—-4.0 cm^{-1}. In our case, the spin exchange coupling constants are in the range of -0.25—1.9 cm^{-1}, indicating both antiferromagnetic and ferromagnetic spin exchange interactions. Clearly, these differences result from the additional phenolato bridge. However, no remarkable difference was observed among the complexes containing L^1, L^2, and L^4. Thus the functional groups on the aromatic rings do not affect the exchange interaction between the Mn^{III} and Mn^{II}.

In summary, the tripodal ligands with an N_2O_2 donor set form the mixed-valence trinuclear complex with the Mn^{III}–Mn^{II}–Mn^{III} arrangement except for the L^3 ligand, which gives only the mononuclear manganese(III) complex. The structure of the complex, mononuclear or trinuclear, is determined by the steric factor of the ligands. The 3-positioned *t*-butyl group on the aromatic rings of the tripodal ligand hinders the bridging of the phenolate oxygen donor. The electronic effect of the ligands makes small contributions to the structural parameters and the magnetic properties.

The authors thank Institute for Molecular Science for the use of a high-sensitivity Faraday balance and diffractometers. The authors also thank Dr. Masahiro Sakai, and Dr. Takashi Fujihara for useful discussions and assistance in the magnetic studies. The present work was supported by Grants-in-Aid for Scientific Research Nos. 05403009 and 07640753 from the Ministry of Education, Science, Sports and Culture.

References

1) V. L. Pecoraro, M. J. Baldwin, and A. Gelasco, *Chem. Rev.*, **94**, 807 (1994).
2) G. Renger, *Angew. Chem., Int. Ed. Engl.*, **26**, 643 (1987).
3) K. Wieghardt, *Angew. Chem., Int. Ed. Engl.*, **28**, 1153 (1989).
4) G. W. Brudvig and R. H. Crabtree, *Prog. Inorg. Chem.*, **37**, 99 (1989).
5) J. B. Vincent and G. Christou, *Adv. Inorg. Chem.*, **33**, 197 (1989).
6) L. Que, Jr., and A. E. True, *Prog. Inorg. Chem.*, **38**, 97 (1990).
7) V. L. Pecoraro, "Manganese Redox Enzymes," VCH, New York (1992).
8) V. K. Yachendra, V. J. DeRose, M. J. Latimer, I. Mukerji, K. Sauer, and M. P. Klein, *Science*, **260**, 675 (1993).
9) E. J. Larson and V. L. Pecoraro, *J. Am. Chem. Soc.*, **113**, 3810 (1991).
10) E. Larson, M. S. Lah, X. Li, J. A. Bonadies, and V. L. Pecoraro, *Inorg. Chem.*, **31**, 373 (1992).
11) J. W. Gohdes and W. H. Armstrong, *Inorg. Chem.*, **31**, 368 (1992).
12) G. C. Dailey, C. P. Horwitz, and C. A. Lisek, *Inorg. Chem.*, **31**, 5325 (1992).
13) C. P. Horwitz, P. J. Winslow, J. T. Warden, and C. A. Lisek, *Inorg. Chem.*, **32**, 82 (1993).
14) C. P. Horwitz, Y. Ciringh, C. Liu, and S. Park, *Inorg. Chem.*, **32**, 5951 (1993).
15) M. R. Bermejo, A. Castiñeiras, J. C. Garcia-Monteagudo, M. Rey, A. Sousa, M. Watkinson, C. A. McAuliffe, R. G. Pritchard, and R. L. Beddoes, *J. Chem. Soc., Dalton Trans.*, **1996**, 2935.
16) H. Torayama, T. Nishide, H. Asada, M. Fujiwara, and T. Matsushita, *Chem. Lett.*, **1996**, 387.
17) C. J. Hinshaw, G. Peng, R. Singh, J. T. Spence, J. H. Enemark, M. Bruck, J. Kristofzski, S. L. Merbs, R. B. Ortega, and P. A. Wexler, *Inorg. Chem.*, **28**, 4483 (1989).
18) "TEXSAN: Single Crystal Structure Analysis Software, Version 1.6," Molecular Structure Corp., The Woodlands, TX 77381 (1993).
19) G. M. Sheldrick, "SHELXS 86 in Crystallographic Computing 3," ed by G. M. Sheldrick, C. Krüger, and R. Goddard, Oxford University Press, Oxford (1985), p. 175.
20) A. Neves, S. M. D. Erthal, I. Vencato, A. S. Ceccato, Y. P. Mascarenhas, O. R. Nascimento, M. Hörner, and A. A. Batista, *Inorg. Chem.*, **31**, 4749 (1992).
21) D. P. Kessissoglou, M. L. Kirk, M. S. Lah, X. Li, C. Raptopoulou, W. E. Hatfield, and V. L. Pecoraro, *Inorg. Chem.*, **31**, 5424 (1992).
22) D. A. Maramatari, P. Hitou, A. G. Hatzidimitriou, F. E. Inscore, A. Gourdon, M. L. Kirk, and D. P. Kessissoglou, *Inorg. Chem.*, **34**, 2493 (1995).
23) V. Tangoulis, D. A. Malamatari, K. Soulti, V. Stergiou, C. P. Raptopoulou, A. Terzis, T. A. Kabanos, and D. P. Kessissoglou, *Inorg. Chem.*, **35**, 4974 (1996).
24) K. Kambe, *J. Phys. Soc. Jpn.*, **5**, 48 (1950).
25) J. B. Vincent, H.-R. Chang, K. Folting, J. C. Huffman, G. Christou, and D. N. Hendrickson, *J. Am. Chem. Soc.*, **109**, 5703 (1987).